NIH Public Access
Author Manuscript
J Pediatr Surg. Author manuscript; available in PMC 2011 June 1.

Published in final edited form as:
J Pediatr Surg. 2010 June ; 45(6): 1246–1255. doi:10.1016/j.jpedsurg.2010.02.093.

Toll-Like Receptor 4 is Protective against Neonatal Murine Ischemia-Reperfusion Intestinal Injury

Philip M. Tatum Jr, MD[†], **Carroll M. Harmon, MD, PhD**[‡], **Robin G. Lorenz, MD, PhD**[§,*], and **Reed A. Dimmitt, MD**[†,‡,1,2]

[†]Department of Pediatrics, University of Alabama at Birmingham

[§]Department of Pathology, University of Alabama at Birmingham

[*]Department of Microbiology, University of Alabama at Birmingham

[‡]Department of Surgery, University of Alabama at Birmingham

Abstract

Purpose—Premature infants receiving probiotics have a decreased incidence of necrotizing enterocolitis. This may be mediated by intestinal bacterial signaling via toll-like receptors (TLRs) 2 and 4 maintaining intestinal homeostasis. We hypothesized that TLRs 2 and 4 are protective against ischemia-reperfusion (I/R) intestinal injury.

Methods—Two-week-old C57BL/6 wild-type (WT), B6.TLR2$^{-/-}$, B6.TLR4$^{-/-}$, B6.TLR2$^{-/-}$4$^{-/-}$, and microbially reduced (antibiotic treated) mice (MR) underwent 60 minutes of superior mesenteric artery occlusion (I) followed by 90 minutes of reperfusion (R). Small intestine was harvested for analysis of microscopic injury, apoptosis, and inflammatory gene expression using quantitative PCR.

Results—Following I/R, the median histological injury scores of the B6.TLR4$^{-/-}$, B6.TLR2$^{-/-}$4$^{-/-}$, and MR pups were higher than the WT or B6.TLR2$^{-/-}$ pups which corresponded with greater apoptosis based on TUNEL and activated caspase-3 immunostaining. B6.TLR4$^{-/-}$, B6.TLR2$^{-/-}$4$^{-/-}$, and MR also had elevated tissue innate immunity associated chemokine and cytokine expression

Conclusions—Neonatal mice deficient in TLR4, either alone or also deficient in TLR2, as well as those lacking a normal commensal intestinal microbiome are more susceptible to an I/R model of intestinal injury. These results may provide a mechanism for commensal bacterial-mediated protection, which may help to direct further studies to elucidate the mechanism of probiotic protection.

[2]This work was supported in part by the NIH grants R01 DK059911, P01 DK071176, K08 HD46506, and the University of Alabama at Birmingham Digestive Diseases Research Development Center Grant P30 DK064400. PT received partial support from the UAB Dixon Fellowship. Aspects of this project were conducted in biomedical research space that was constructed with funds supported in part by the NIH grant C06RR020136.

© 2010 Elsevier Inc. All rights reserved.

[1]Address correspondence to: Dr. Reed A. Dimmitt, Department of Pediatrics, University of Alabama at Birmingham, 1600 7th Avenue South, ACC 618, Birmingham, AL 35233. rdimmitt@uab.edu Ph: 205.939.9918. Fax: 205.939.9919.

Publisher's Disclaimer: This is a PDF file of an unedited manuscript that has been accepted for publication. As a service to our customers we are providing this early version of the manuscript. The manuscript will undergo copyediting, typesetting, and review of the resulting proof before it is published in its final citable form. Please note that during the production process errors may be discovered which could affect the content, and all legal disclaimers that apply to the journal pertain.

NIH-PA Author Manuscript
NIH-PA Author Manuscript
NIH-PA Author Manuscript

NIH-PA Author Manuscript

NIH-PA Author Manuscript

NIH-PA Author Manuscript

Keywords

Toll-like receptors; necrotizing enterocolitis; microbiota; ischemia-reperfusion

Introduction

Necrotizing enterocolitis (NEC) continues to be associated with significant morbidity and mortality in very low birth weight (VLBW) infants [1]. Recent clinical trials have indicated that probiotics may reduce the risk of NEC [2]. The rationale for probiotics arises from the theory that VLBW infants almost uniformly receive broad spectrum antimicrobial therapy with delay in feedings, resulting in an abnormal intestinal microbiota. A potential mechanism of probiotic associated NEC prevention is that these bacteria maintain intestinal homeostasis by signaling through host toll-like receptors (TLRs). TLRs are innate immune molecules that function as receptors for specific bacterial and viral ligands [3]. Adult mice deficient in TLRs have been shown to have increased experimental colitis [4] and NEC [5] but there is a paucity of studies pertaining to neonatal models of NEC.

The aim of our study was to determine the role of TLR2 and TLR4, the receptors for bacterial ligands associated with Gram positive and negative bacteria, respectively, in an ischemia/reperfusion (I/R) model of NEC in neonatal mice. In addition, mouse pups receiving broad-spectrum antimicrobial medication similar to that experienced in the early postnatal period of VLBW infants underwent I/R. We hypothesized that 2-week-old mice deficient in TLR2, TLR4, TLR2 and 4, and those with a reduced intestinal microbiota would have greater I/R intestinal injury compared to wild-type mice with a normal microbiota. Specifically, we hypothesized that the experimental groups would have increased mucosal necrosis, apoptosis, and increased expression of inflammatory immune molecules.

Methods

Mice

Adult C57BL/6 wild-type, B6.TLR2$^{-/-}$, B6.TLR4$^{-/-}$, and B6.TLR2$^{-/-}$4$^{-/-}$ mice were used for breeding to obtain 2-week-old pups for the study. The B6.TLR2$^{-/-}$ and B6.TLR4$^{-/-}$ were provided as gift from Drs. Shizuo Akira at Osaka University Japan and Doug Golenbock at the University of Massachusetts. The mice with combined TLR2 and 4 deficiencies were bred at our facility and screened by PCR using the primer sequences: for TLR2, GGTTCAAGCCCCTTTCTTCTTTA (forward), TGTGAGATGAGAAAAAAGAGATGTTTC (reverse); for TLR4, CAGAGTTTCCTGCAATGGATCA (forward), TGCTTATCTGAAGGTGTTGCACAT (reverse). The breeders were raised under specific pathogen free (SPF) conditions, and acclimatized to our facility 2 weeks prior to mating. The pups were born and housed under conventional conditions and nursed until time of sacrifice. Experiments were approved by the Institutional Animal Care and Use Committee of the University of Alabama at Birmingham, approval number 081107653. A list of SPF conditions is available at http://main.uab.edu/sites/ComparativePathology/surveillance/.

Microbial Reduction

Antibiotics were added to the drinking water using a modification of Hans, et al [6]. Adult C57BL/6 wild-type microbially reduced (MR) animals were maintained with the addition of streptomycin sulfate (4.8 mg/mL), ampicillin (1.2mg/mL), metronidazole (1.2mg/mL), and vancomycin (0.6mg/mL) (Sigma, St. Louis, MO) to sterile drinking water *ad libitum* and

NIH-PA Author Manuscript

NIH-PA Author Manuscript

NIH-PA Author Manuscript

changed bi-weekly. Females were treated 5 days prior to mating and antibiotic therapy continued throughout the experimental period.

Analysis of fecal samples by PCR-Denaturing gradient gel electrophoresis (PCR-DGGE)

DNA extraction of fecal samples obtained from 2-week-old WT and MR pups was used for PCR-DGGE analysis as previously described [7]. Primers were used for PCR amplification targeting different variable regions of the 16S rRNA. The forward primer sequence was ACTACGTGCCAGCAGCCCGCCGGGCCGCGGCCCGCCCGCCCGCGGGGGCACGG GGGACTACGTGCCAGCAGCC and the reverse sequence was GGACTACCAGGGTATCTAATCC. Analysis of PCR products was performed using a gradient denaturant gel which was scanned using a GS-710 Calibrated Imaging Densitometer® (Bio-Rad Inc., Hercules, CA). Selected bands were excised from the gel and DNA extracted via a crush soak process. The DNA was used for an additional PCR using the above primers joined to M13 vector sequences as previously described [8] and the sequence analyzed using the online Ribosomal Database Project provided by the Center for Microbial Ecology at Michigan State University (http://rdp.cme.msu.edu/).

Induction of Ischemia-Reperfusion (I/R) Injury

After achieving adequate anesthesia with inhaled oxygen and isofluorane (MWI, Meridian, ID) delivered via a Vapomatic™ vaporizer (A.M. Bickford, Inc, Wales Center, NY), midline laparotomy was performed on 2-week-old C57BL/6 wild-type (WT), TLR 2 $^{-/-}$, TLR 4 $^{-/-}$, TLR 2$^{-/-}$ 4 $^{-/-}$, and MR mice. Ischemia was achieved by placing a 4 cm straight micro-serrefine aneurysm clamp (Fine Science Tools,, Inc. Foster City, CA) across the superior mesenteric artery as previous described [9]. The laparotomy was closed using a single simple continuous suture of 3-0 silk (Ethicon, Inc, Somerville, NJ). After 60 minutes of ischemia, the clamp was removed and laparotomy closed as previous described. The mice were sacrificed after 90 minutes of reperfusion using an overdose of inhaled isoflurane and death confirmed by cervical dislocation. Segments of the mid-jejunum were harvested and placed in Bouin's fixative solution (Fisher Scientific, Kalamazoo, MI) and RNA*l*ater®(Ambion, Inc., Austin, TX) for histological and real time polymerase chain reaction (RT-PCR) analyses, respectively.

Two-week-old mice from each cohort were used as mock treated controls for the I/R animals. These mice did not undergo anesthesia or laparotomy. Following sacrifice, the tissue was harvested and processed as mentioned above.

Injury Scoring

Portions of mid-jejunum were embedded in paraffin, microtome-sectioned, and stained with hematoxylin and eosin (Sigma-Aldrich, St. Louis, MO) for analysis of I/R mediated injury. The scoring range was 0 to 5 using a modified scoring system reported by Jilling, et al based on depth of injury; 0-no injury; 1-vacuolization only; 2-villous tip; 3-mid-villous; 4-entire crypt; 5-to the muscularis layer [10]. The scoring was independently performed by two authors (PT, RD) in a masked fashion. A composite injury score was based on multiple scores from five separate histologic sections of intestine for each mouse and reported as the median injury score.

TUNEL Immunostaining

The presence of apoptotic cells was determined by using the ApopTag® kit (Millipore Corp, Billerica, MA) for terminal deoxynucleotidyl transferase-mediated dUTP-FITC nick-end labeling (TUNEL), which labels characteristic DNA breaks associated with apoptosis. Mid-jejunal sections were deparaffinized and underwent antigen retrieval using a heated solution of citric acid and sodium citrate. Following protein digestion with Proteinase K (Sigma-

NIH-PA Author Manuscript

NIH-PA Author Manuscript

NIH-PA Author Manuscript

Aldrich, St. Louis, MO), the slides were treated with TUNEL reaction solution to label the DNA fragments with digoxigenin-nucleotide and incubated for 1 hour at 37°C. Fluorescein conjugated anti-digoxigenin antibody was then added to slides for 30 minutes in the dark followed by application of Hoechst (Sigma-Aldrich, St. Louis, MO) dye for non-specific nuclear staining.

Activated caspase-3 Immunostaining

To determine the specific apoptotic pathway involved in I/R injury, activated caspase-3 immunostaining was performed. Sections of mid-jejunum were deparaffinized and underwent antigen retrieval using heated Target Retrieval Solution, High pH™ (Dako, Inc, Carpinteria, CA). Endogenous peroxidase was blocked with 3% hydrogen peroxide in phosphate buffered solution (PBS) for 10 minutes. After blocking for endogenous biotin activity with Avidin/ Biotin Blocking Kit (Vector Laboratories Inc, Burlingame, CA) the sections were treated with a primary rabbit monoclonal anti-mouse activated caspase-3 antibody (Invitrogen Corp, Carlsbad, CA), diluted to 1:500 in PBS+1% bovine serum albumin, 0.3% Triton®-X-100 and 0.2% powdered milk(PBS-BB) (Fisher Scientific Inc, Fair Lawn, NJ). The slides were incubated overnight at 4°C in a humidity chamber. PBS-BB alone was added to control slides. The biotin-conjugated donkey anti-rabbit IgG secondary antibody (Jackson ImmunoResearch Inc, West Grove, PA) was diluted to 1:1000 in PBS-BB and added to the slides for 1 hour at room temperature. Streptavidin conjugated horseradish peroxidase (Jackson ImmunoResearch Inc, West Grove, PA) was diluted at 1:1000 in PBS-BB and added to the slides for 30 minutes. Fluorescence amplification was performed using TSA™ Plus Cyanine 3 (PerkinElmer, Waltham, MA) at 1:1000 for 30 minutes in the dark. Slides were counterstained with Hoechst dye (Sigma-Aldrich, St. Louis, MO) for non-specific nuclear staining.

Apoptosis Quantification

Five representative digital images at 100× magnification were taken of activated caspase-3 stained slides from each of the groups using a Zeiss Axioskop 2 mot plus microscope equipped with fluorescence imaging filters and Zeiss Axiocam™ (Carl Zeiss IMT Corporation, Maple Grove, MN). Brightness was set manually to eliminate background noise and ensure similarity between images. Using Metamorph® (MDS Analytical Technologies, Sunnyvale, CA), total activated caspase-3 staining was determined and expressed as fluorescence intensity. Fluorescence intensity was defined as a percent of field of view above a set brightness threshold for caspase uptake. All intestinal segments from the groups were similar in size and therefore direct comparison could be made between groups.

RNA isolation and gene expression

Sections of mid-jejunum from mock and I/R treated mice were harvested and placed in RNA*later*®(Ambion, Inc., Austin, TX) for analysis of the expression of inflammatory molecules. RNA was isolated using Trizol® as described {Chomczynski, 1987}(Invitrogen®, Carlsbad, CA). Genomic DNA contamination was removed using the Turbo DNA-*free* kit available from Applied Biosystems® (Foster City, CA). RNA was transcribed into cDNA using Roche's Transcriptor First Strand cDNA Synthesis Kit® (Pensburg, Germany). Real-time reverse transcription polymerase chain reaction (RT-PCR) was performed using TaqMan Universal PCR Mix® (Invitrogen®, Carlsbad, CA) in combination with Applied Biosystems® primer probe sets. Specific gene RNA levels were determined using crossing thresholds read by the RT cycler MX3000P® (Stratagene®, La Jolla, CA), and expressed as a log difference from initial fluorescence detection. Fluorescence thresholds were averaged generating a gene specific numeral which then could be normalized to the average expression of the 18S housekeeping gene and further stratified by particular strain and experimental condition. Gene expression was calculated as an average fold change when compared to control strain values,

NIH-PA Author Manuscript

NIH-PA Author Manuscript

NIH-PA Author Manuscript

and shown on a log 2 scale as fold changes from the control baseline (=1). The protocol for this data analysis format is provided in the Applied Biosystems manufacturer's instructions (4371095 Rev A, PE Applied Biosystems).

Statistical analysis

Sigma Stat 2.03 (SPSS Inc., Chicago, IL 60606 USA) software was used for data analysis. Student's t-test and one-way ANOVA were used for continuous variables, and Fisher's exact test was used for categorical variables. Non-parametric analysis was performed with a Mann-Whitney test. Gene expression differences were analyzed using Student's test to compare ΔΔCT and standard deviation between the experimental and control animals. A p value < 0.05 was regarded as significant.

Results

Microbial reduction using antibiotics

To assess the degree of microbial reduction in the mice receiving antibiotic therapy, MR and SPF 2-week-old mice were analyzed for the presence of bacteria using amplification of 16s rRNA. After DNA extraction and PCR with conserved bacterial 16s rRNA primers, a DGGE analysis revealed a relatively diverse microbial population in the SPF feces (Figure 1, Lanes D,E) compared to MR mice (Figure 1, Lanes A–C). A band denoting a single bacterial species was observed in the MR mice (Figure 1, arrow). Sequence analysis revealed this band corresponded with *Pseudomonas aeruginosa* that had a 93% sequence similarity when queried using the Ribosomal Database Project. Thus, the mice reared by dams receiving antimicrobial therapy had a marked reduced commensal bacterial diversity with the selection of a single Gram negative organism.

Ischemia reperfusion intestinal injury

Previous work has shown that adult mice lacking TLRs have greater morbidity and mortality in a model of colitis and our laboratory has shown that adult B6.TLR2$^{-/-}$ mice have greater I/R induced intestinal injury compared to WT mice. Thus, we hypothesized that neonatal mice deficient in these same bacterial signaling molecules would have increased I/R injury. To determine which TLRs are important in I/R protection, C57BL/6 WT, B6.TLR2$^{-/-}$, B6.TLR4$^{-/-}$, and B6.TLR2$^{-/-}$4$^{-/-}$ were studied. Figure 2 (A–F) represents the histological findings used for injury scoring (injury score of 0–5, respectively). The pathological findings are primarily coagulation necrosis and intestinal villous sloughing, similar to what is present in human NEC tissue. The median Figure 1 histological injury scores were significantly higher in the B6.TLR 4$^{-/-}$ and B6.TLR2$^{-/-}$4$^{-/-}$ mice compared to WT mice (Figure 2, G, median 3 versus. 2). MR mice showed a tendency toward higher injury scores (median 3 versus. 2), but did not achieve significance. The B6.TLR2 $^{-/-}$ mice had similar injury scores to WT with a median injury score of 1. Taken together, these data show that neonatal mice deficient in the LPS signaling molecule TLR4 have greater I/R injury than WT mice and mice with a reduced commensal microbial diversity trended toward greater injury.

Apoptosis

While the H&E findings show evidence of necrosis, I/R injury is also associated with increased apoptosis [10]. We next set out to determine the role of apoptosis in our model of NEC. Examination of intranuclear TUNEL staining (Figure 3, B) following I/R revealed subjectively increased apoptosis in B6.TLR4$^{-/-}$, B6.TLR2$^{-/-}$4$^{-/-}$, and MR mice (Figure 3, D–F, respectively) while the WT and B6.TLR2$^{-/-}$ mice had minimal apoptotic cells (Figure 3, A, B). To determine the possible apoptotic pathway associated with I/R injury, sections of small intestines obtained from the various cohorts were analyzed for the presence of activated

NIH-PA Author Manuscript

NIH-PA Author Manuscript

NIH-PA Author Manuscript

caspase-3 (Figure 4, B). Subjectively, there was greater activated caspase-3 staining in the B6.TLR4$^{-/-}$, B6.TLR2$^{-/-}$4$^{-/-}$, and MR mice (Figure 4, D–F, respectively), corresponding to the TUNEL staining results. Computer aided quantitative analysis of the mean fluorescence intensity confirmed that there were significantly higher amounts of activated caspase-3 in these strains compared to the WT controls. Thus, these experiments demonstrate that the MR and mice deficient in TLR4 have greater I/R medicated apoptosis, a possible mechanism of the increased tissue injury.

Baseline analysis of inflammatory molecule gene expression

We next set out to determine the role of inflammatory mediators in both protection from I/R injury as well as the role of these cytokines and chemokines in the mechanism of disease. We hypothesized that mice lacking TLR would have less inflammatory mediator gene expression than WT mice. Table 1 shows the results of RT-PCR analysis of 16 cytokines and chemokines associated with intestinal inflammation. There was no difference in any of these molecules between the WT controls and the B6.TLR2$^{-/-}$, B6.TLR4$^{-/-}$, or B6.TLR2$^{-/-}$4$^{-/-}$ mice. In contrast, the MR mice had greater expression of Interleukin-23 (IL-23a), interferon-gamma (IFN-γ), and myeloperoxidase (MPO) when normalized to the WT mice but not in the other inflammatory molecules. Thus, mice deficient in TLR2, 4, or both had similar baseline small intestinal inflammation prior to I/R. While the MR mice had greater IL-23a, IFN-γ, and MPO expression, the expression of the classic innate inflammatory molecules was similar to that of WT mice, including IL-6 as well as chemokines bearing the glutamic acid-leucine-arginine and cysteine-amino acid-cysteine (ELR+ CXC) motif. These chemokines are the mouse equivalent of human IL-8. Specifically, there was no significant difference in small intestinal LPS-inducible CXC chemokine (CXCL5, LIX), macrophage inflammatory protein-2 (CXCL2, MIP-2), and keratinocyte-derived chemokine (CXCL1, KC).

Innate and adaptive inflammatory molecules following I/R

Since NEC is an acute intestinal disease and our model results in rapid injury, we hypothesized the mice with more severe intestinal injury would have greater expression of innate inflammatory mediators. Following I/R, the B6.TLR4$^{-/-}$ mice had increased expression of MIP-2 and IL-6 while the B6.TLR2$^{-/-}$4$^{-/-}$ mice had greater LIX, MIP-2, KC, IL-1α, and IL-6 expression compared to the WT controls (Figure 5). In addition, the MR also had increased inflammatory gene expression (MIP-2, IL-6) while the expression of the innate inflammatory mediators in the B6.TLR2$^{-/-}$ was not significantly different than that of the WT mice.

When we analyzed the expression of cytokines associated with adaptive immune function, we found no difference in IL-4 expression between the TLR deficient mice and the WT controls but a significantly greater IL-4 and IFN-γ expression in the MR mice. In addition, the B6.TLR4$^{-/-}$ mice had increased expression of IL-10 while the B6.TLR2$^{-/-}$4$^{-/-}$ mice had more IL-2, IL-10 and IL-23a expression (Figure 6).

Taken together, these results demonstrate a link between the degree of I/R injury and inflammatory mediator expression. Specifically, neonatal mice deficient in either TLRs or normal commensal bacteria have an increase in tissue chemokine production compared to WT.

Discussion

NEC continues to be a leading cause of morbidity and mortality in very low birth weight (VLBW) infants. Despite advances with other illnesses of VLBW infants, the rate of NEC remains unchanged over the last 2 decades [11]. Lack of insight into the mechanism of NEC has made development of treatments aimed at preventing the disease difficult. While the pathogenesis in NEC is likely multifactorial, key factors that have been implicated in NEC

NIH-PA Author Manuscript

NIH-PA Author Manuscript

NIH-PA Author Manuscript

include intestinal hypoperfusion [12], abnormal bacterial colonization [13], a dysregulated immune response [14,15] and feeding [16].

The intestinal environment is considered sterile at birth, and during the neonatal period bacteria from the environment are acquired and make up the scaffolding for the intestinal microbiome [17]. The intestinal mucosal immune system develops tolerance at least in part through commensal intestinal bacterial stimulation of TLRs [18]. TLRs are transmembrane components of the innate immune system's pattern recognition receptor family [3]. Through recognition of bacterial products, intestinal TLRs maintain homeostasis by balancing the pro-inflammatory and anti-inflammatory immune responses to both commensal and pathogenic microbiota. Dysregulation of this immune response has been implicated in inflammatory bowel diseases [19] and may also play a key role in the pathogenesis of NEC.

Animal models have previously shown the protective role of toll-like receptors and their downstream components. Mice lacking TLRs or MyD88, the signaling molecule associated with TLRs, as well as microbially reduced mice that are devoid of bacteria necessary to signal intestinal TLRs have been shown to have significantly worse damage in a dextran sulfate sodium (DSS) model of colitis. However, when these microbially reduced mice are given lipoteichoic acid (LTA) and lipopolysaccharide (LPS), which stimulate TLR2 and TLR4 respectively, they are completely protected from DSS-induced mortality [4].

Recent clinical studies have indicated that enteral probiotics decrease the risk of NEC in some VLBW infants, though the exact mechanism remains unknown. Premature infants have abnormal intestinal colonization due to altered environmental bacteria and administration of antibiotics, which have been shown to functionally down regulate TLR expression (Dimmitt, 2009, submitted for publication). The healthy microbiome that is normally acquired postnatally is replaced with a pathogenic one that may direct the intestinal immune system to a more pro-inflammatory state. Studies have speculated that probiotic TLR signaling to dendritic cells plays a role in immunomodulation and tolerance via induction of immunosuppressive regulatory T cells [20]. Moreover, simultaneous stimulation of both TLR2 and TLR4 has been shown to have a synergistic effect on the production of anti-inflammatory cytokines [21]. Therefore, the protection from NEC conferred by probiotics may function through TLRs.

In the current study, we sought to further examine the protective effects of stimulation of TLRs 2 and 4 in an ischemia reperfusion model of NEC in hopes of further elucidating the mechanism of protection seen with probiotic administration. While the injury induced in this model is similar to established NEC models, it should be noted that this is an ischemia-reperfusion model rather than a NEC model. Our findings confirm previous studies showing that mice unable to signal through TLRs 2 and 4 have increased susceptibility to mucosal damage. Microbially reduced mice that lack the microbiome to signal TLRs and are analogous to VLBW infants undergoing antibiotic treatment [10] trended toward worse injury and had increased apoptosis.

As evidenced by our immunostaining, apoptosis was a mechanism of mucosal injury. Similar to findings by Jilling, we found that apoptosis likely occurred prior to intestinal necrosis, thus explaining the increased luminal TUNEL and caspase-3 markers. Tight junction proteins have been shown to initiate apoptosis [23], and TLRs induce expression of certain tight junction proteins [24]. Thus, in the normal host, stimulation of TLRs by intestinal bacteria may play a role in reducing susceptibility to damage and subsequent apoptosis.

The exaggerated inflammatory response that we found in TLR deficient and MR mice may be responsible for further worsening ischemia-reperfusion induced damage. Our lab has previously shown that adult B6.TLR2 deficient mice have worse ischemia-reperfusion induced intestinal injury when compared to WT mice [5]. The current study in neonatal mice found no difference between mucosal injury between B6.TLR 2 $^{-/-}$ and WT mice. This may reflect a

NIH-PA Author Manuscript

NIH-PA Author Manuscript

NIH-PA Author Manuscript

differential expression of TLRs in neonatal mice compared to adult mice which may be related to the acquisition of microbiota. The establishment of the microbiome begins first with colonization by facultative anaerobic Gram negative bacteria, thus bacterial signaling of TLR4 predominates in the neonatal gut [17]. It is not until later when true anaerobic Gram positive bacteria are acquired that would be sensed by TLR2. As the gut acquires bacteria in the neonatal period, there is a relative down regulation of TLRs to adult levels [25,26]. This down regulation prevents an exaggerated inflammatory response to acquired bacteria; however a low level expression is likely necessary for normal gut development. The increased inflammatory response in TLR $2^{-/-}4^{-/-}$ mice compared to TLR $4^{-/-}$ mice indicates that cross-talk between TLRs may promote low-level expression, and it may be the loss of this balance between the developmental role and inflammatory role of TLRs that is responsible for increased mucosal damage. A reduction in bacterial diversity resulting from antibiotic use potentially promotes an imbalance in TLR expression, thus altering intestinal homeostasis.

Our results regarding the tissue expression of innate inflammatory mediators is in agreement with other investigators, indicating an acute injury process [15]. In addition, there were mixed results regarding the adaptive inflammatory mediators, with no significant increased expression of IL-17 but more IL-23a in the B6.TLR$2^{-/-}4^{-/-}$ pups. The finding of increased IL-10, a regulatory and anti-inflammatory cytokine, in the strains with greater I/R injury was unexpected. A previous study has shown that increased tissue IL-1 results in increased IL-10 following intestinal I/R injury and may explain our results as the mice with greater IL-10 expression had greater IL-1α expression.[27].

In summary, neonatal mice deficient in TLR4, either alone or in concert with TLR2, as well as mice lacking a diverse intestinal commensal microbiome are more susceptible to intestinal mucosal damage. Thus, the presence of commensal bacterial TLR signaling may lead to improved early intestinal homeostasis.

Acknowledgments

We would like to thank Jamie McNaught, and the Cell and Molecular Pathology Core of the Digestive Disease Developmental Center at UAB for assistance with the histology, Peggie McKie-Bell for animal husbandry assistance, and Randy Bullock for his assistance with the RT-PCR and PCR-DGGE experiments.

References

1. Lemons J, Bauer C, Oh W, et al. Very low birth weight outcomes of the National Institute of Child health and human development neonatal research network, January 1995 through December 1996. NICHD Neonatal Research Network. Pediatrics 2001;107:E1. [PubMed: 11134465]
2. Alfaleh K, Bassler D. Probiotics for prevention of necrotizing enterocolitis in preterm infants. Cochrane Database Syst Rev. 2008 CD005496.
3. Barton G, Kagan J. A cell biological view of Toll-like receptor function: regulation through compartmentalization. Nat Rev Immunol 2009;9:535–542. [PubMed: 19556980]
4. Rakoff-Nahoum S, Paglino J, Eslami-Varzaneh F, et al. Recognition of commensal microflora by toll-like receptors is required for intestinal homeostasis. Cell 2004;118:229–241. [PubMed: 15260992]
5. Aprahamian C, Lorenz R, Harmon C, et al. Toll-like receptor 2 is protective of ischemia-reperfusion-mediated small-bowel injury in a murine model. Pediatr Crit Care Med 2008;9:105–109. [PubMed: 17906593]
6. Hans W, Schölmerich J, Gross V, et al. The role of the resident intestinal flora in acute and chronic dextran sulfate sodium-induced colitis in mice. Eur J Gastroenterol Hepatol 2000;12:267–273. [PubMed: 10750645]
7. Simpson J, Martineau B, Jones W, et al. Characterization of fecal bacterial populations in canines: effects of age, breed and dietary fiber. Microb Ecol 2002;44:186–197. [PubMed: 12087428]

NIH-PA Author Manuscript

NIH-PA Author Manuscript

NIH-PA Author Manuscript

8. O'Sullivan L, Webster G, Fry J, et al. Modified linker-PCR primers facilitate complete sequencing of DGGE DNA fragments. J Microbiol Methods 2008;75:579–581. [PubMed: 18789360]
9. Dimmitt R, Glew R, Colby C, et al. Serum cytosolic beta-glucosidase activity in a rat model of necrotizing enterocolitis. Pediatr Res 2003;54:462–465. [PubMed: 12867598]
10. Jilling T, Lu J, Jackson M, et al. Intestinal epithelial apoptosis initiates gross bowel necrosis in an experimental rat model of neonatal necrotizing enterocolitis. Pediatr Res 2004;55:622–629. [PubMed: 14764921]
11. Fanaroff A, Hack M, Walsh M. The NICHD neonatal research network: changes in practice and outcomes during the first 15 years. Semin Perinatol 2003;27:281–287. [PubMed: 14510318]
12. Nankervis C, Giannone P, Reber K. The neonatal intestinal vasculature: contributing factors to necrotizing enterocolitis. Semin Perinatol 2008;32:83–91. [PubMed: 18346531]
13. Claud E, Walker W. Hypothesis: inappropriate colonization of the premature intestine can cause neonatal necrotizing enterocolitis. FASEB J 2001;15:1398–1403. [PubMed: 11387237]
14. Sibbons P, Spitz L, van Velzen D. Necrotizing enterocolitis induced by local circulatory interruption in the ileum of neonatal piglets. Pediatr Pathol 12:1–14. [PubMed: 1561146]
15. Frost B, Jilling T, Caplan M. The importance of pro-inflammatory signaling in neonatal necrotizing enterocolitis. Semin Perinatol 2008;32:100–106. [PubMed: 18346533]
16. Berseth C. Feeding strategies and necrotizing enterocolitis. Curr Opin Pediatr 2005;17:170–173. [PubMed: 15800406]
17. Adlerberth I, Wold A. Establishment of the gut microbiota in Western infants. Acta Paediatr 2009;98:229–238. [PubMed: 19143664]
18. Zeuthen L, Fink L, Frøkiaer H. Toll-like receptor 2 and nucleotide-binding oligomerization domain-2 play divergent roles in the recognition of gut-derived lactobacilli and bifidobacteria in dendritic cells. Immunology 2008;124:489–502. [PubMed: 18217947]
19. Abreu M. Immunologic regulation of toll-like receptors in gut epithelium. Curr Opin Gastroenterol 2003;19:559–564. [PubMed: 15703605]
20. Foligne B, Zoumpopoulou G, Dewulf J, et al. A key role of dendritic cells in probiotic functionality. PLoS One 2007;2:e313. [PubMed: 17375199]
21. Hirata N, Yanagawa Y, Ebihara T, et al. Selective synergy in anti-inflammatory cytokine production upon cooperated signaling via TLR4 and TLR2 in murine conventional dendritic cells. Mol Immunol 2008;45:2734–2742. [PubMed: 18372043]
22. Lin H, Hsu C, Chen H, et al. Oral probiotics prevent necrotizing enterocolitis in very low birth weight preterm infants: a multicenter, randomized, controlled trial. Pediatrics 2008;122:693–700. [PubMed: 18829790]
23. Nava P, Laukoetter M, Hopkins A, et al. Desmoglein-2: a novel regulator of apoptosis in the intestinal epithelium. Mol Biol Cell 2007;18:4565–4578. [PubMed: 17804817]
24. Cario E, Gerken G, Podolsky D. Toll-like receptor 2 enhances ZO-1-associated intestinal epithelial barrier integrity via protein kinase C. Gastroenterology 2004;127:224–238. [PubMed: 15236188]
25. Naik S, Kelly E, Meijer L, et al. Absence of Toll-like receptor 4 explains endotoxin hyporesponsiveness in human intestinal epithelium. J Pediatr Gastroenterol Nutr 2001;32:449–453. [PubMed: 11396812]
26. Melmed G, Thomas L, Lee N, et al. Human intestinal epithelial cells are broadly unresponsive to Toll-like receptor 2-dependent bacterial ligands: implications for host-microbial interactions in the gut. J Immunol 2003;170:1406–1415. [PubMed: 12538701]
27. Souza D, Guabiraba R, Pinho V, et al. IL-1-driven endogenous IL-10 production protects against the systemic and local acute inflammatory response following intestinal reperfusion injury. J Immunol 2003;170:4759–4766. [PubMed: 12707357]

NIH-PA Author Manuscript

NIH-PA Author Manuscript

NIH-PA Author Manuscript

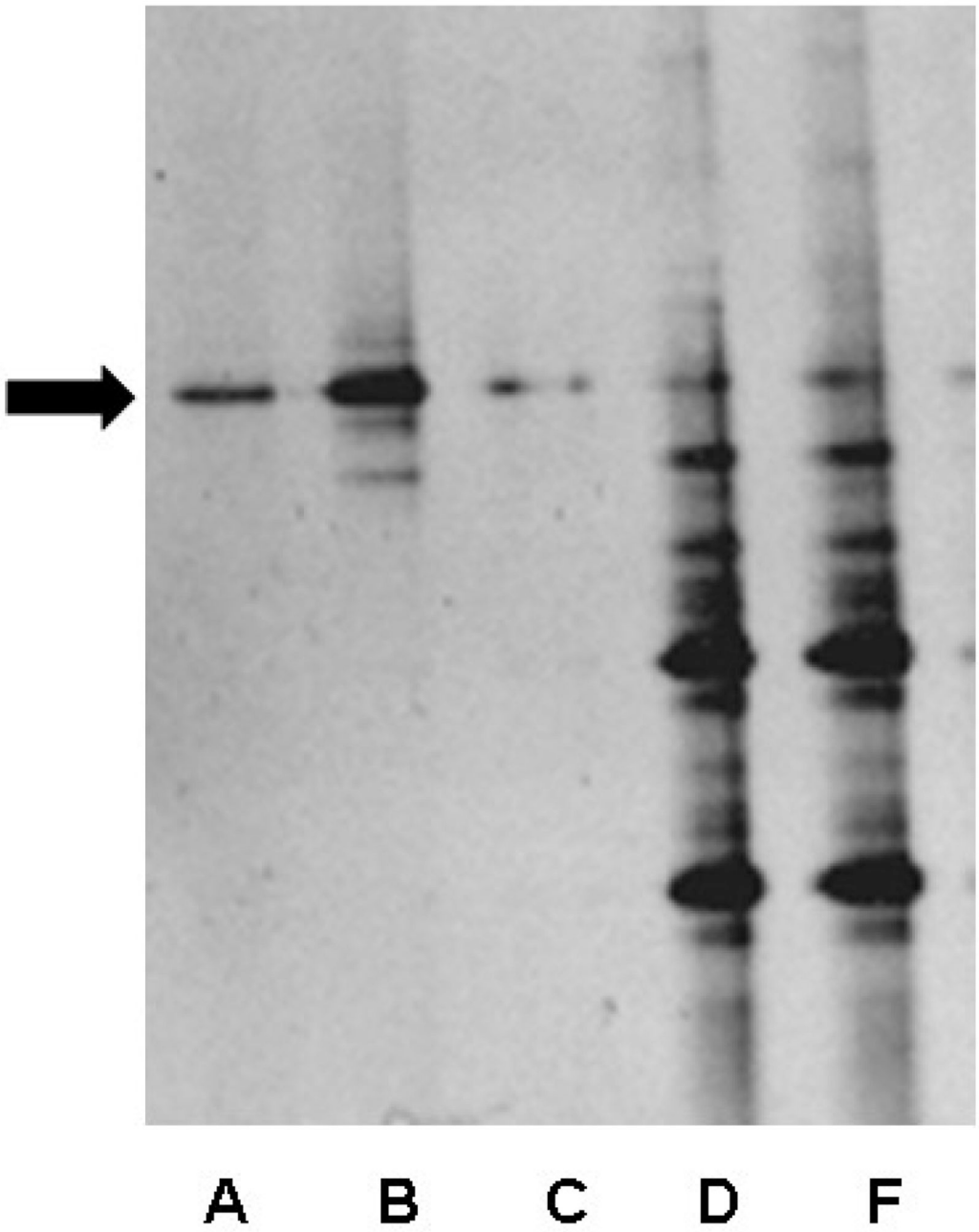

Figure 1.
PCR-DGGE analysis of feces from 2-week-old MR and WT mice. Lanes A, B, C =MR, lanes D, F= WT. The black arrow indicates persistent banding pattern observed in the MR mice.

NIH-PA Author Manuscript

NIH-PA Author Manuscript

NIH-PA Author Manuscript

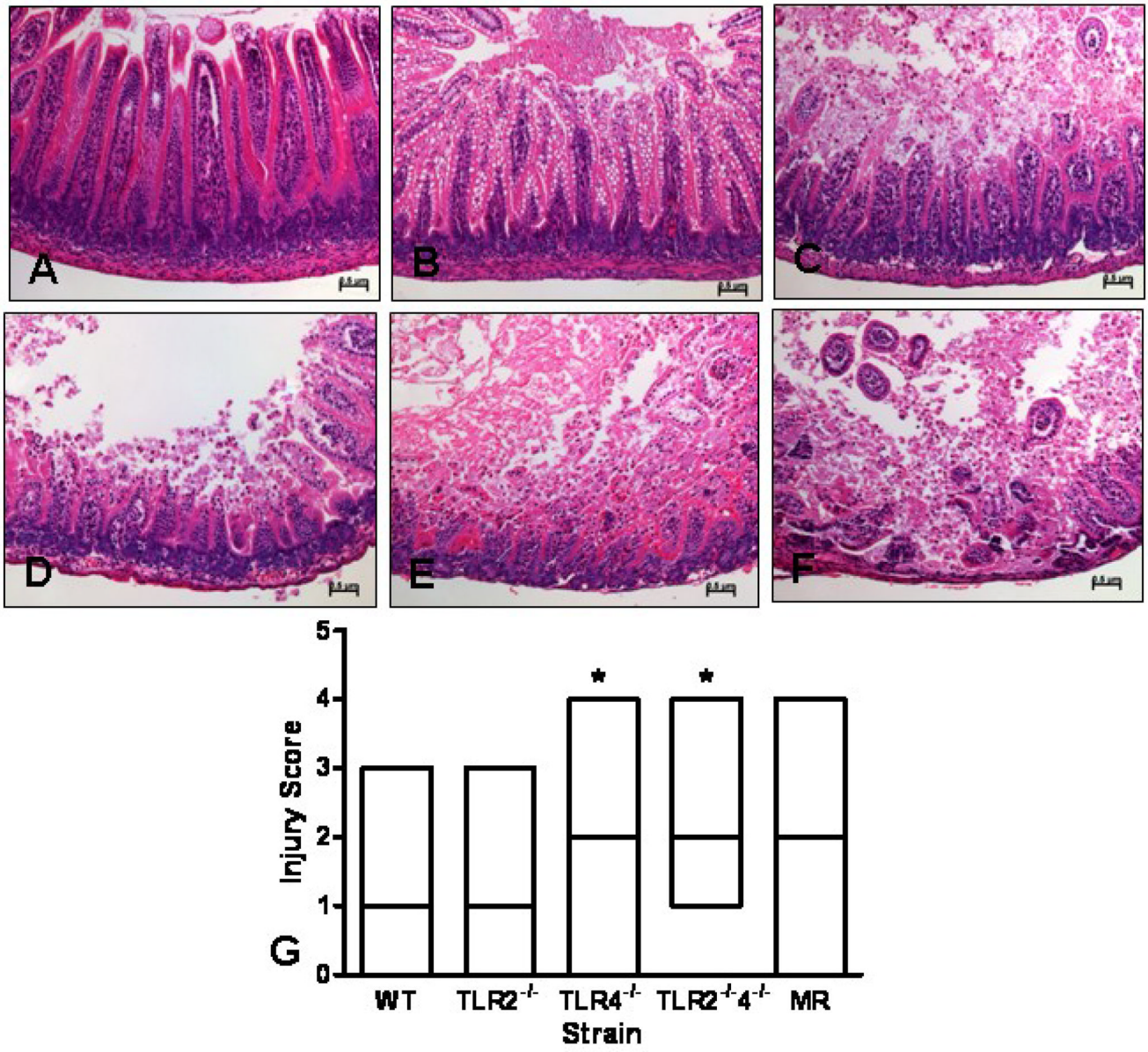

Figure 2.

Histological injury scores following I/R injury. The scoring range was 0 to 5 using a modified scoring system reported by Jilling [10] based on depth of injury; 0-no injury(A); 1-vacuolization (B); 2-villous tip (C); 3-mid-villous (D); 4-entire crypt (E); 5-to the muscularis layer (F). The images were photographed at 200× magnification. The median score for each strain was analyzed by ANOVA, *$p<0.05$ (G). n=10 animals per strain.

NIH-PA Author Manuscript

NIH-PA Author Manuscript

NIH-PA Author Manuscript

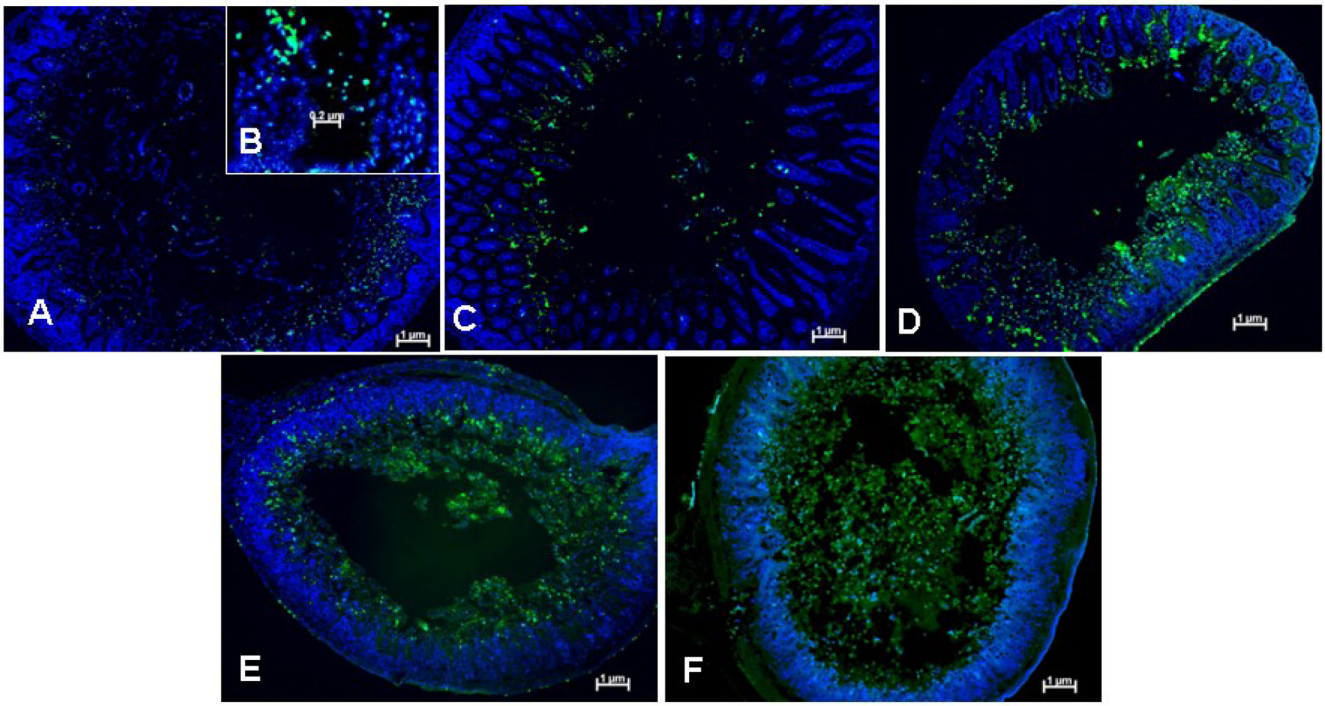

Figure 3.

TUNEL immunostaining following I/R injury. Each image is representative of the degree of TUNEL positive cells for each strain (A) WT, (C) B6.TLR2$^{-/-}$, (D) B6.TLR4$^{-/-}$, (E) TLR2$^{-/-}$4$^{-/-}$, (F) MR. at 100× magnification. (B) 200× image demonstrating intranuclear TUNEL staining indicative of apoptosis. Green=TUNEL, blue=Hoechst

NIH-PA Author Manuscript
NIH-PA Author Manuscript
NIH-PA Author Manuscript

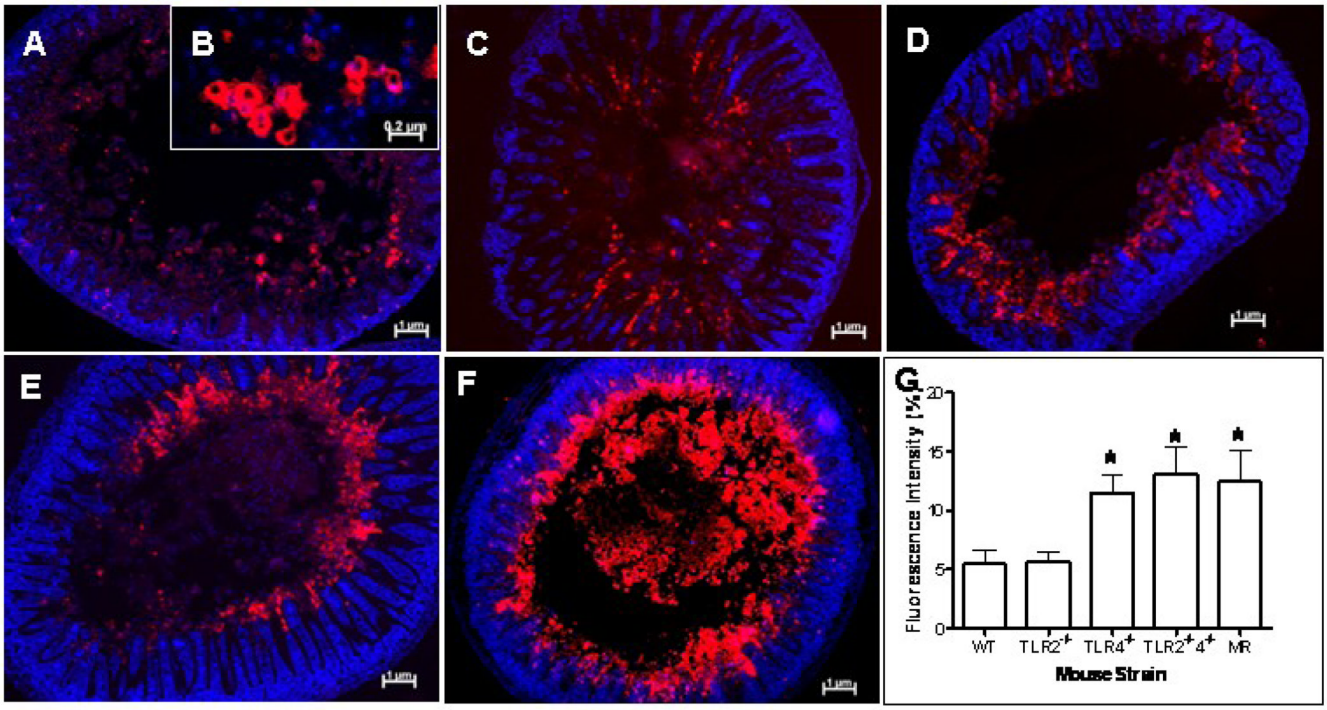

Figure 4.

Activated caspase-3 immunostaining following I/R injury. Each image is representative of the degree of activated caspase-3 positive cells for each strain (A) WT, (C) B6.TLR2$^{-/-}$, (D) B6.TLR4$^{-/-}$, (E) TLR2$^{-/-}$4$^{-/-}$, (F) MR. at 100× magnification. (B) 200× image demonstrating activated caspase-3 staining. Red=caspase-3, blue=Hoechst. (G) Mean fluorescence intensity of activated caspase-3 staining for each strain, analyzed by ANOVA, *p<0.05. n=5 animals per strain

NIH-PA Author Manuscript

NIH-PA Author Manuscript

NIH-PA Author Manuscript

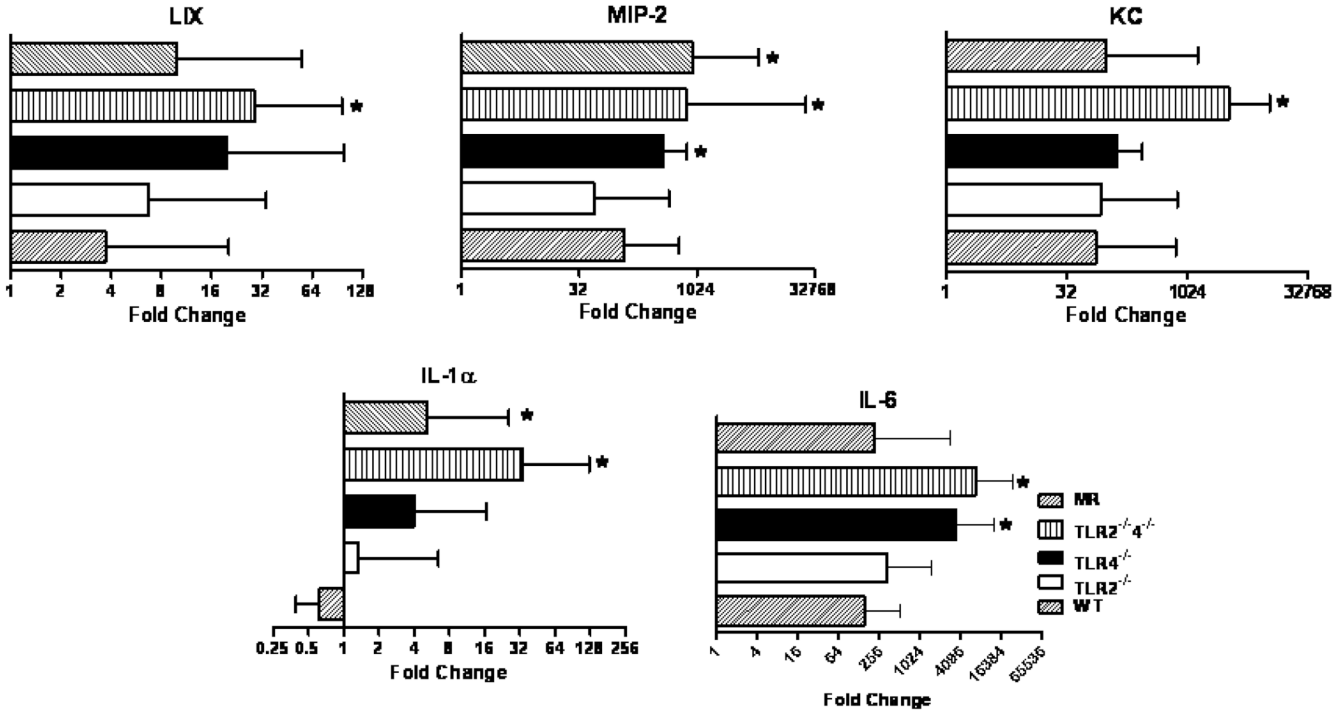

Figure 5.

Quantitative RT-PCR analysis of innate immune molecule expression in I/R injury by strain. RT-PCR data is expressed in $\log_2$ scale and normalized to 18S rRNA expression with ΔΔCT calculated comparing I/R to mock control, analyzed by ANOVA, *p<0.05., n=10 animals per strain

NIH-PA Author Manuscript

NIH-PA Author Manuscript

NIH-PA Author Manuscript

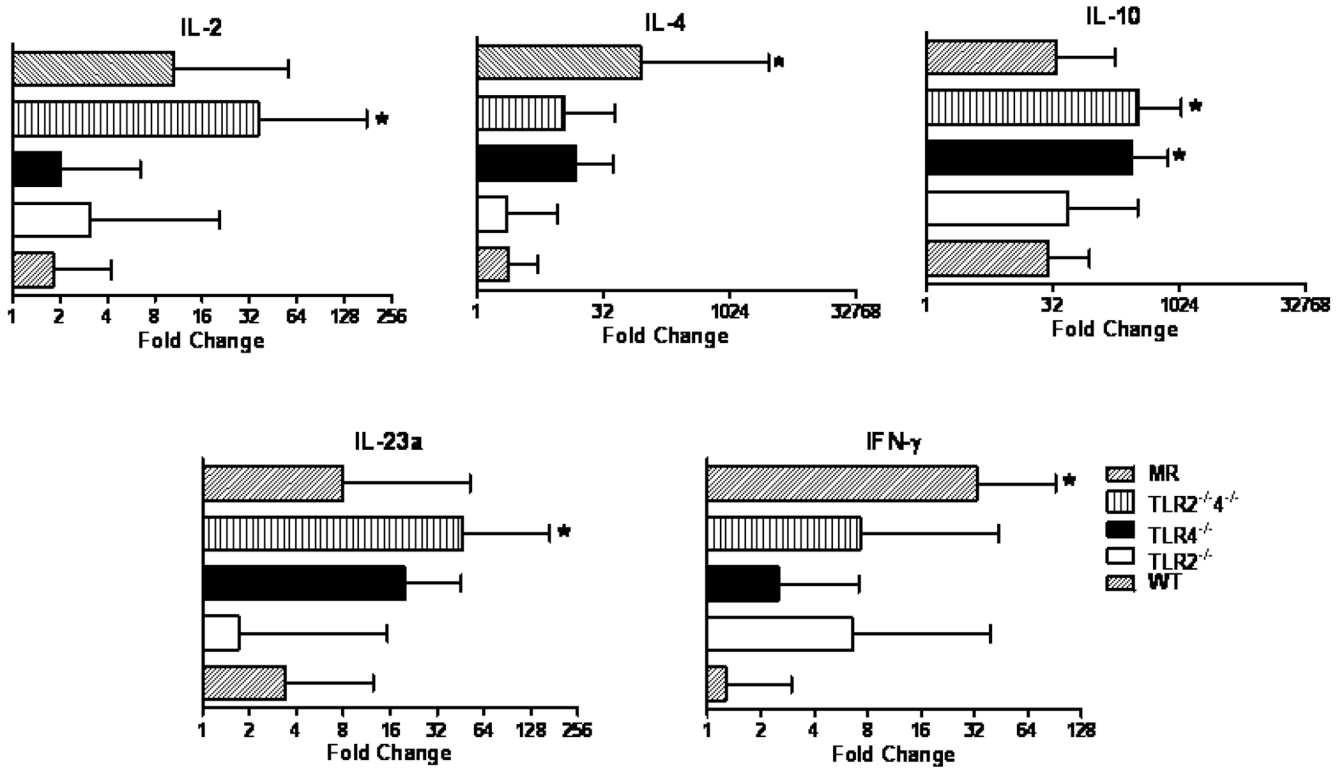

Figure 6.

Quantitative RT-PCR analysis of adaptive immune molecule expression in I/R injury by strain. RT-PCR data is expressed in $\log_2$ scale and normalized to 18S rRNA expression with ΔΔCT calculated comparing I/R to mock control, analyzed by ANOVA, *p<0.05., n=10 animals per strain

NIH-PA Author Manuscript NIH-PA Author Manuscript NIH-PA Author Manuscript

Table 1

Comparison of baseline intestinal cytokine and chemokine expression in 2-week-old mock control mice. The values are expressed as fold change and range in each strain compared to WT pups. NS-non-significant

Cytokine	TLR $2^{-/-}$ (=10)	TLR $4^{-/-}$ (n=10)	TLR $2^{-/-}4^{-/-}$ (n=10)	MR (n=10)	P value
IL-1α	0.26 (0.09–0.79)	0.35 (0.06–2.10)	0.15 (0.05–0.42)	0.28 (0.05–1.55)	NS
IL-2	0.48 (0.06–3.96)	0.78 (0.34–1.8)	0.15 (0.06–0.37)	0.30 (0.07–1.30)	NS
IL-4	1.20 (0.14–10.21)	0.46 (0.19–1.13)	0.32 (0.11–0.90)	2.06 (0.40–10.74)	NS
IL-6	1.18 (0.16–8.66)	1.30 (0.22–7.83)	0.10 (0.04–0.22)	2.41 (0.53–10.94)	NS
IL-10	0.68 (0.18–2.60)	0.31 (0.06–1.49)	0.14 (0.06–0.35)	4.41 (1.39–13.95)	NS
IL-17	2.22 (1.09–4.52)	2.32 (0.73–7.40)	1.62 (0.97–2.71)	3.14 (0.88–11.26)	NS
IL-22	3.70 (1.13–12.16)	1.82 (0.58–5.68)	1.40 (0.83–2.34)	3.72 (0.91–15.24)	NS
IL-23a	2.46 (0.55–11.04)	0.80 (0.10–6.36)	0.18 (0.05–0.66)	21.35 (4.02–113.39)*	*p<0.05
IFN-γ	1.92 (0.84–4.39)	1.96 (0.52–7.40)	1.49 (0.82–2.70)	15.88 (1.93–130.50)*	*p<0.05
TGF-β	0.65 (0.08–5.43)	0.29 (0.05–1.75)	0.32 (0.07–1.51)	0.41 (0.10–1.72)	NS
TNF-α	0.45 (0.27–0.73)	0.51 (0.11–2.28)	0.37 (0.15–0.95)	0.68 (0.22–2.08)	NS
LIX	0.45 (0.27–0.73)	0.46 (0.08–2.63)	0.27 (0.10–0.73)	1.99 (0.70–5.65)	NS
KC	0.49 (0.08–3.0)	1.14 (0.30–4.36)	0.09 (0.02–0.52)	3.83 (0.93–15.79)	NS
MIP-2	1.46 (0.89–2.39)	0.33 (0.05–2.14)	0.14 (0.01–1.28)	0.45 (0.04–4.63)	NS
Lungkine	0.87 (0.31–2.43)	0.30 (0.11–0.81)	0.14 (0.05–0.36)	0.34 (0.06–2.50)	NS
MPO	3.53 (2.18–5.69)	1.10 (0.37–3.32)	0.63 (0.40–1.01)	8.94 (3.35–23.85)*	*p<0.05